Surface Science 118 (1982) 1–18
North-Holland Publishing Company

SPECTROSCOPIC ELLIPSOMETRIC INVESTIGATION OF CLEAN AND OXYGEN COVERED COPPER SINGLE CRYSTAL SURFACES

L.J. HANEKAMP, W. LISOWSKI * and G.A. BOOTSMA

Department of Applied Physics, Twente University of Technology, P.O. Box 217, 7500 AE Enschede, The Netherlands

Received 6 January 1982; accepted for publication 9 March 1982

Spectroscopic ellipsometric measurements (400–820 nm) have been performed on clean and oxygen covered Cu(110) and Cu(111) surfaces in an AES–LEED UHV system. The complex dielectric functions of the clean surfaces were calculated from measurements between room temperature and 600 K. In contrast with Cu(111), for the Cu(110) surface the ellipsometric parameters Δ and ψ depend on the azimuth of the plane of incidence of the light beam. Such an anisotropy was also found for the changes in Δ and ψ measured upon adsorption of oxygen to coverages corresponding with approximately 1/2 and 1 monolayer. To explain the results, several models are discussed, in which changes with substrate optical properties are taken into account.

1. Introduction

With the combination ellipsometry–AES–LEED, Habraken et al. have observed linear relations between the change in the ellipsometric parameter Δ at $\lambda = 632.8$ nm and the oxygen coverage θ in the chemisorption stage on Cu(111) [1], Cu(100) [2] and Cu(110) [3,4] ($\theta \lesssim 0.5$ oxygen atoms per surface metal atom). After this stage a further uptake takes place, accompanied by reconstruction of the surface. For the anisotropic Cu(110) plane, the ellipsometric effects $\delta\Delta$ and $\delta\psi$ appeared to depend on the crystal temperature and on the azimuth, Ω, of the plane of incidence ($\Omega = 0°$: plane of incidence parallel to $[\bar{1}10]$) [3,5]. To explain the results, several models were proposed in which changes in the substrate optical properties, caused by chemisorption, are taken into account [5].

In order to facilitate the interpretation and use of ellipsometric measurements in the study of chemisorption and the initial stage of oxidation, spectroscopic ellipsometric measurements of clean and oxygen covered metal surfaces are being carried out. In this paper, we report upon measurements with copper surfaces in the wavelength region 400–820 nm at temperatures between 295 and 600 K. To elucidate the observed optical anisotropy, the

* Research-Fellow at Twente University of Technology.

0039-6028/82/0000–0000/$02.75

measurements were performed with the anisotropic Cu(110) and the isotropic Cu(111) plane at different azimuth of the plane of incidence.

2. Experimental

The experiments were performed in an ion-pumped stainless steel UHV system provided with facilities for AES/LEED and ellipsometry. The vacuum system and the origin and pretreatment of the samples were essentially the same as described in ref. [6]. In the course of the experiments the valve, which could separate the ion pump from the system, was removed to avoid contamination of the rest gas by degassing of the viton gasket after several bake-out cycles. After this removal, the power supply of the ion pump was switched off during the dynamical cleaning and exposure cycles. To avoid contamination of the oxygen gas and to reduce the straylight during the optical measurements, the pressure in the system was measured with an ionization gauge at the turbo-molecular pump. At pressures between 10^{-4} to 10^{-8} Torr, the ratio between the pressure in the reaction chamber and at the turbo-molecular pump appeared to be constant (~ 5.0).

A schematic diagram of the polarizer-sample-rotating analyser-fixed analyser ($PSA_{rot}A$) ellipsometer that has been built in our laboratory is given in fig. 1. The rotating analyser is speed-controlled [7] with an accuracy within 5 ppm at an angular frequency of 66.6 Hz. The harmonic detector signal is fed into a filter circuit where two frequencies are separated as described in refs. [7,8]. The ellipsometric parameters Δ and ψ are calculated from the measured phase angles of the two frequencies. The program for this calculation is loaded in the microprocessor from a cassette recorder. Two programs are available; one calculates Δ and ψ in one zone and provides a plot on the recorder of these parameters as a function of time, the other gives Δ and ψ in two zones and their averaged value on the terminal display. For the definition of the zones, see ref. [9]. In principle, Δ and ψ could be measured after one revolution of the rotating analyser. To get a higher accuracy, the Δ and ψ values were de-

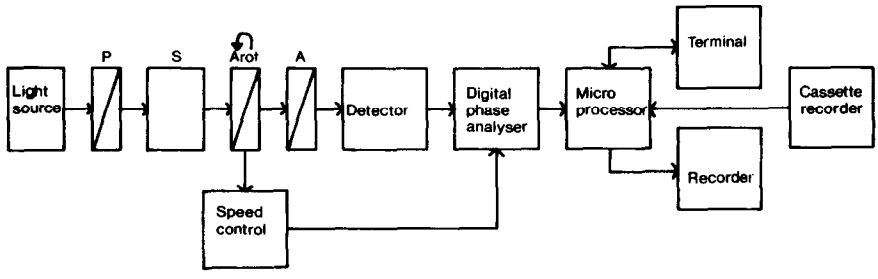

Fig. 1. Schematic diagram of the $PSA_{rot}A$ ellipsometer.

termined by averaging over at least 900 revolutions. As a light source a 100 W halogen lamp combined with a monochromator (Leiss, model D 330) with slit widths of 0.5 mm was used. For alignment, the lamp was replaced by a He–Ne laser. A lens (focal length 20 cm) and several pin holes were mounted after the monochromator to get a parallel beam with a diameter of about 1 mm at the sample. For the detector an end-on photomultiplier with an S-20 response (EMI, type 9659 QB) was used.

The optical components were placed on two optical benches, which were each fixed on a disc (Micro Controle, type TR 160 combined with MR 160.80) with high precision rotation and translation facilities. The discs and the UHV system were mounted on a frame. To enable the determination of the plane of incidence with the alignment procedure of McCrackin et al. [10], with a reflecting metal surface outside the UHV chamber, both discs could rotate in the same plane. The vacuum chamber was provided with two sets of Pyrex windows; with one set the crystal surface could be positioned such that AES/LEED and ellipsometric measurements could be carried out without altering the position of the sample (cf. ref. [11]); the other set at the opposite side was used in the present study.

The ellipsometric measurements were performed in zone 1 and 2 in the wavelength region 400–820 nm, at intervals of 20 nm. All the measurements were performed at an angle of incidence of $66.00 \pm 0.05°$. During the wavelength scans, the position of the sample was controlled after every 5–6 measuring points by determining Δ and ψ at 632.8 nm.

The presented values reported for Δ, ψ, $\delta\Delta$ and $\delta\psi$ ($\delta\Delta \equiv \bar{\Delta} - \Delta$ and $\delta\psi \equiv \bar{\psi} - \psi$, $\bar{\Delta}$, $\bar{\psi}$: clean surface) are averages of at least two series of measurements. The accuracy in the average values appeared to be of the same order as in the individual results ($\pm 0.03°$).

To eliminate the influence of the birefringence of the ellipsometer windows on the absolute values of $\bar{\Delta}$ and $\bar{\psi}$, correction factors were determined from measurements with oxygen covered surfaces with and without windows as a function of the wavelength at 1 atm N_2 pressure. After introduction of the N_2 gas in the system it took approximately 1 h before Δ and ψ became constant. These measurements were always carried out before demounting the crystal.

3. Clean copper surfaces

3.1. Determination of dielectric constants

The investigation of clean surfaces by spectroscopic ellipsometry yields the optical constants n and k, or ϵ' and ϵ'' as a function of the wavelength. The complex optical constant and complex dielectric constant are given by

$$\tilde{n} = n - ik, \tag{1}$$

$$\tilde{\epsilon} = \epsilon' - i\epsilon'' = n^2 - k^2 - i2nk. \tag{2}$$

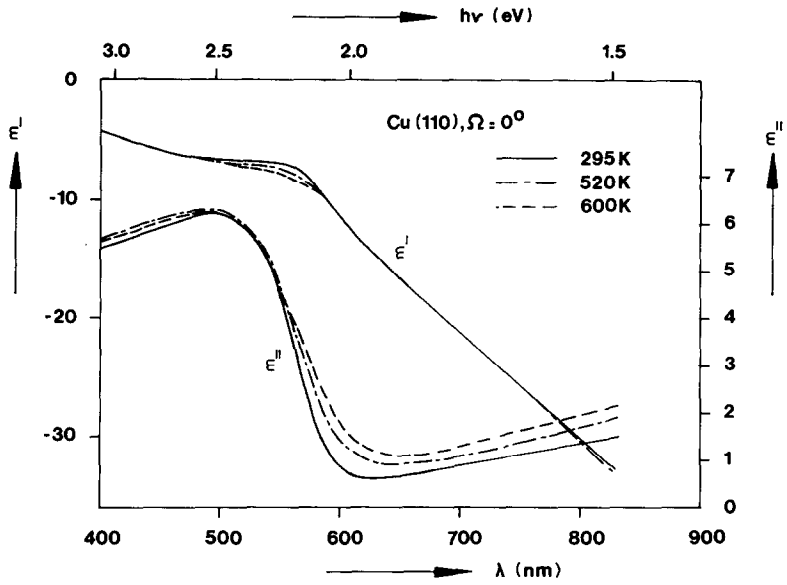

Fig. 2. The components of the complex dielectric function for Cu(110), $\Omega = 0°$ calculated from $\bar{\Delta}$, $\bar{\psi}$ data at 295, 520 and 600 K.

The computer program of McCrackin [12] was used to calculate the optical constants from $\bar{\Delta}$ and $\bar{\psi}$. In fig. 2, the dielectric constants ϵ' and ϵ'' for Cu(110), $\Omega = 0°$, are plotted as a function of the wavelength for different sample temperatures. The same measurements were performed for Cu(110), $\Omega = 90°$ and for Cu(111) at two azimuths of the plane of incidence, parallel and perpendicular to a $\langle \bar{1}10 \rangle$ direction. For both orientations on Cu(111), ϵ' and ϵ'' appeared to be within the experimental error identical and equal to the results obtained for Cu(110), $\Omega = 0°$.

3.2. Experimental errors

The optical constants of clean surfaces are derived from absolute values of the ellipsometric parameters Δ and ψ. Systematic experimental errors have therefore a larger influence than in the recording of relative changes $\delta\Delta$ and $\delta\psi$ during a process taking place at the reflecting surface. In this section we focus on errors with respect to angle of incidence, cleanliness of surface and window birefringence.

(i) To illustrate the influence of errors in the angle of incidence, ϕ_0, we have calculated effective values of the real and imaginary part of the complex dielectric function of copper from the experimental data of Cu(110), $\Omega = 0°$, $T = 295$ K by assuming a change in the angle of incidence of $\pm 1°$. Fig. 3 shows

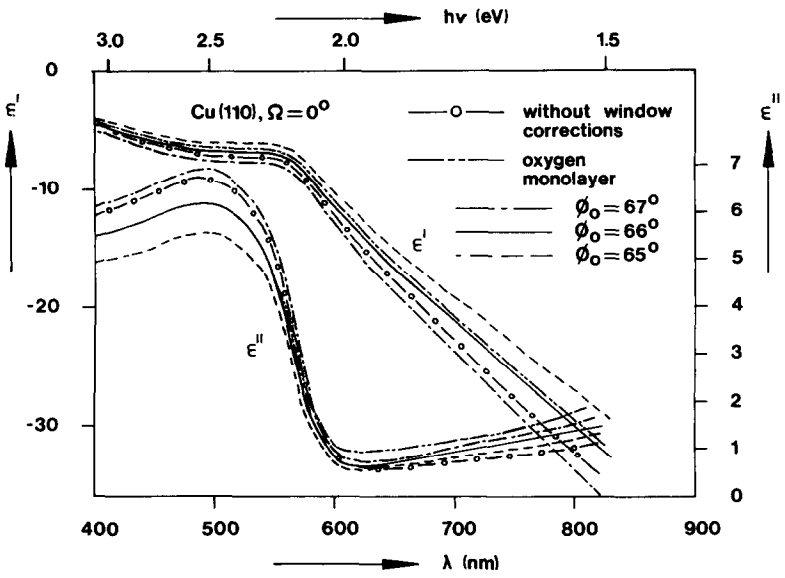

Fig. 3. Effective values of the components of the dielectric function for Cu(110), $\Omega = 0°$ calculated from (i) the $\bar{\Delta}$ and $\bar{\psi}$ values measured at $\psi_0 = 66°$, for different angles of incidence; (ii) the measured $\bar{\Delta}$ and $\bar{\psi}$ values ignoring window corrections; (iii) Δ and ψ values corresponding to about one monolayer of oxygen.

that the corresponding changes in the effective values of $|\epsilon'|$ and ϵ'' are on the order of $\pm 10\%$ in the wavelength region studied. In our case, the experimental errors in ϕ_0 are on the order of $\pm 0.05°$; for our examples this implies errors in ϵ' and ϵ'' of about 0.5%.

(ii) The effect of neglecting the presence of a surface layer is also shown in fig. 3, for Cu(110) covered with about 1 monolayer of chemisorbed oxygen. Effective values of ϵ' and ϵ'' were calculated from the Δ and ψ values measured after the adsorption of an amount of oxygen corresponding with the c(6 × 2) structure (cf. section 4). At photon energies above the band gap (> 2.2 eV) the influence of such a thin layer is negligible but at lower energies the changes in $|\epsilon'|$ and ϵ'' are on the order of 2% an 30%, respectively.

(iii) The corrections for window birefringence, determined as described in section 2, appeared to be considerable. An example of the influence on the dielectric constants is given in fig. 3, showing that the corrected and uncorrected values are clearly different. The corrections were not the same for the different samples and/or orientations, due to differences in mounting and baking of the windows and in extent of the chemical reaction on the surface. Because the angle of incidence could be measured with a high accuracy and the cleanliness of the surface was controlled by AES, the accuracy of $\bar{\Delta}$ and $\bar{\psi}$ is mainly determined by errors in the correction for window birefringence.

3.3. Comparison with literature

In fig. 4 the components of ϵ for Cu(110), $\Omega = 0°$ and 90°, are compared with published values obtained at room temperature. Roberts [13] determined the optical properties of annealed and electropolished polycrystalline copper samples by means of ellipsometry. The measurements were done with the sample in a vacuum of about 2×10^{-5} Torr after removal of the oxide layer by heating to a temperature of 500 K. Stoll [14] determined the optical constants with a different polarimetric method for a polycrystalline sample in a vacuum of 5×10^{-7} Torr. The final cleaning was achieved by heating to 525 K under a pressure of 10^{-4} Torr of pure hydrogen. The results are in good agreement with those of Roberts [13] and have therefore been omitted in fig. 4. Pells and Shiga [15] tried to improve the surface cleanliness of their polycrystalline samples by preheating to higher temperatures (~ 900 K) in high vacuum and by measuring in ultra-high vacuum ($\sim 10^{-9}$ Torr). Their ϵ'' values are not significantly different from those of Johnson and Christy [16,17] plotted in fig. 4.

The results of Johnson and Christy were obtained from reflection and transmission measurements on vacuum-evaporated, unannealed films, which had been exposed to air. Merkt and Wissmann [18] prepared thin copper films by evaporation under UHV conditions and obtained optical constants by ellipsometric measurements with unannealed films in UHV. Their data are in

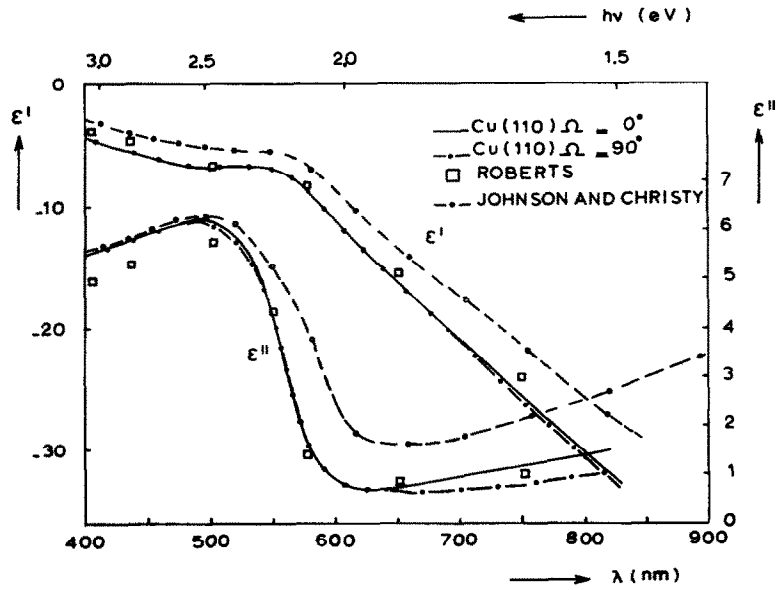

Fig. 4. The components of the complex dielectric function for copper: Cu(110), $\Omega = 0°$ and $\Omega = 90°$; annealed bulk polycrystal in UHV [13]; unannealed thin film [16,17].

accord with those of Johnson and Christy. Bispinck [19] measured the influence of the annealing temperature on the ellipsometrically determined optical constants of thick copper films in UHV. His results obtained with films annealed at the highest temperature (600 K) agree well with those of Roberts; for films annealed at lower temperatures, the values of ϵ' and ϵ'' shift in the direction of those determined by Johnson and Christy.

3.4. Anisotropy of clean Cu(110)

In principle, one expects even a clean surface to exhibit anisotropy if the site symmetry contains no fourfold or higher order symmetry axis [5]. Thus the clean Cu(110) surface could show optical anisotropy, i.e. different $\bar{\Delta}$ and/or $\bar{\psi}$ values if the crystal is rotated along an axis normal to the surface, in contrast with the Cu(111) surface. In fig. 5, the difference in $\bar{\Delta}$ and $\bar{\psi}$ for the two orientations of the plane of incidence is plotted as a function of wavelength at different temperatures. In view of the errors in absolute measurements (section 3.2), the absolute values of $\delta\bar{\Delta}$ and $\delta\bar{\psi}$ are open to doubt. However, the shape and temperature dependence of the curves in fig. 5 appeared not to be influenced by the window corrections and the structure in the region 500–700 nm was absent in the results for the Cu(111) surface.

With ellipsometry, optical anisotropy has been measured at thick oxide films (10–200 nm) on Cu(110) and Cu(311), where it was ascribed to aniso-

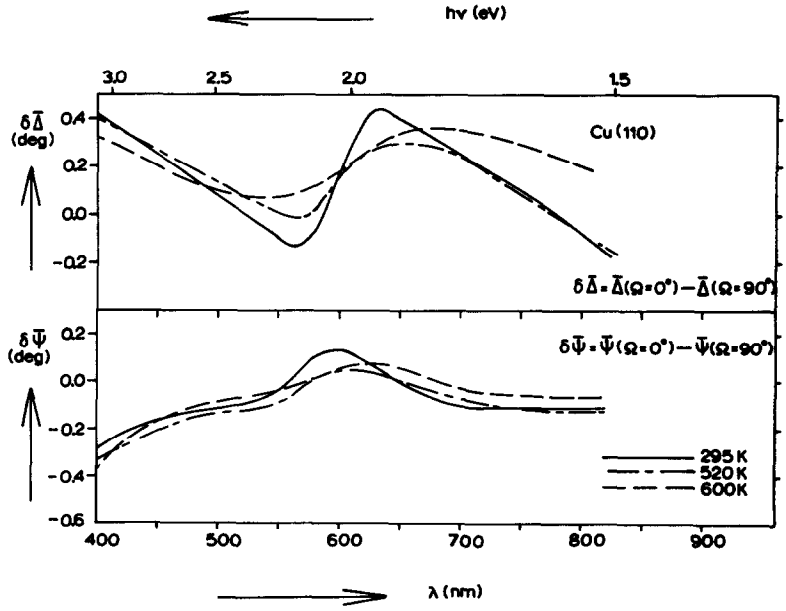

Fig. 5. Difference in ellipsometric parameters $\bar{\Delta}$ and $\bar{\psi}$ for Cu(110) at $\Omega = 0°$ and 90°, $\phi_0 = 66°$.

tropic strain in the oxide film [20]. Optical anisotropy has also been observed by electroreflectance measurements on Ag(110) [21] and on Cu(110) and Au(110) [22,23] in electrolytic solution and by surface plasmon excitation on Ag(110) [24] in contact with air and electrolytic solutions. In these papers, the anistropy was ascribed to direction dependence of the surface conductivity [24], and of the electron (optical) mass [23]. As will be shown below, a calculation of the dielectric constants from the observed $\bar{\Delta}$ and $\bar{\psi}$ value, points in the same direction.

In the classical treatment of the dielectric constant of a metal two contributions are distinguished, that of free and of bound electrons (cf. ref. [25])

$$\tilde{\epsilon} = \tilde{\epsilon}_f + \tilde{\epsilon}_b. \tag{3}$$

For a free electron metal with damping,

$$\tilde{\epsilon}_f(\nu) = 1 - \nu_1^2/(\nu^2 + \nu_2^2) - i(\nu_2/\nu)\,\nu_1^2/(\nu^2 + \nu_2^2). \tag{4}$$

Here ν is the frequency of the light, ν_1 the plasma frequency and ν_2 the electron collision frequency. The plasma frequency is related to the density, N_f, the optical mass, m^*, and the charge, e, of the free electrons:

$$\nu_1^2 = e^2 N_f/4\pi^2\epsilon_0 m^* \quad \text{(SI units)}, \tag{5}$$

where ϵ_0 is the permittivity of vacuum. The collision frequency is given by

$$\nu_2 = 1/2\pi\tau = \nu_1^2/2\sigma_0^*. \tag{6}$$

Here τ is the collision time and σ_0^* the (optical) conductivity. For metals like copper, the collision frequency $\nu_2 \approx 5 \times 10^{12}$ s^{-1} [25] and thus in the visible region of the spectrum $\nu^2 \gg \nu_2^2$. Neglecting ν_2^2 with respect to ν^2, eqs. (3) and (4) reduce to

$$\epsilon'(\lambda) = 1 - (\nu_1^2/c^2)\,\lambda^2 + \epsilon_b', \tag{7}$$

$$\epsilon''(\lambda) = (\nu_2\nu_1^2/c^3)\,\lambda^3 + \epsilon_b'', \tag{8}$$

with $\nu = c/\lambda$ (c: velocity of light). By plotting ϵ' and ϵ''/λ versus λ^2, or e.g. by linear regression analysis of the experimental data, ν_1, ν_2, ϵ_b' and ϵ_b''/λ may be determined.

Though this treatment is only valid for homogeneous isotropic substrates, we have applied it to our measurements on the anisotropic Cu(110) and isotropic Cu(111) surfaces at longer wavelengths, outside the absorption band region. In table 1, the results are given and compared with literature values of Roberts for polycrystalline bulk copper [13[and of Johnson and Christy for copper films [16,17]. The linear regression analysis of our data was carried out for the wavelength region 660–820 nm, while the measurements of Roberts and Johnson and Christy were performed in the regions 650–2500 nm and 700–1940 nm, respectively. Since for Cu(111) the results for the two orientations were the same within the experimental error, the optical parameters have been calculated from the averaged values of ϵ' and ϵ''.

Table 1
Optical parameters of copper

Sample	T (K)	$\nu_1 \times 10^{-15}$ (s^{-1}) ± 0.01	$\nu_2 \times 10^{-12}$ (s^{-1}) ± 0.5	ϵ_b' ± 0.4	ϵ_b''/λ ± 0.07
Cu(110), [$\bar{1}$10]	295	2.33	13.8	7.3	−0.07
	520	2.34	18.0	7.5	−0.16
	600	2.26	20.5	5.6	−0.02
Cu(110), [001]	295	2.36	7.9	8.2	0.17
	520	2.37	13.0	8.4	−0.04
	600	2.28	19.6	6.5	−0.15
Cu(111)	295	2.33	19.4	7.2	−0.68
	520	2.34	20.3	8.8	−0.31
Bulk [13]	90	2.18	5.5	5	0.50
	300	2.18	7.8	5	0.65
	500	2.15	10.9	5	0.80
Film [16,17]	78	2.08	14.1	4.7	0.95
	293	2.11	23.2	5.7	0.63
	423	2.17	32.9	8.6	0.01

A significant conclusion from table 1 is that ν_2 and, according to eq. (6), also τ and σ_0^* are dependent on the nature and temperature of the sample. Moreover, Cu(110) shows a dependence on the orientation, which disappears at higher temperatures.

A more appropriate model for clean Cu(110), e.g. with an isotropic copper substrate ($\tilde{\epsilon}_2$) covered by a biaxially anisotropic surface layer with thickness d_1, contains more parameters ($\tilde{\epsilon}_2$, $\tilde{\epsilon}_{1x}$, $\tilde{\epsilon}_{1y}$, $\tilde{\epsilon}_{1z}$ and d_1) than can be determined from the four experimental quantities. A qualitative insight into the factors that determine the degree of anisotropy can be obtained with Strachan's approach [26,27]. Here, the interfacial layer is represented by a two-dimensional distribution of Hertzian oscillators, characterized by the scattering indices σ_x, σ_y (both parallel to the phase boundaries) and σ_z (perpendicular to them, plane of incidence xz). Expressions for $\delta\Delta$ and $\delta\psi$ due to the presence of an absorbing layer have been given in ref. [5] for $\sigma_x \neq \sigma_y \neq \sigma_z$, with $\sigma_j = \sigma_j' - i\sigma_j''$:

$$\delta\Delta = a_x'\sigma_x' + a_y'\sigma_y' + a_z'\sigma_z' + a_x''\sigma_x'' + a_y''\sigma_y'' + a_z''\sigma_z'', \tag{9}$$

$$\delta\psi = b_x'\sigma_x' + b_y'\sigma_y' + b_z'\sigma_z' + b_x''\sigma_x'' + b_y''\sigma_y'' + b_z''\sigma_z''. \tag{10}$$

The coefficients a_j', a_j'', b_j' and b_j'' depend on $\tilde{\epsilon}_2$, λ and ϕ_0 according to eqs. (23) and (24) of ref. [5]. Since rotation of the plane of incidence over 90° implies only the interchange of x and y components, we get for

$$\begin{aligned}\delta\bar{\Delta} &\equiv \bar{\Delta}(\Omega = 0°) - \bar{\Delta}(\Omega = 90°) \\ &= -(a_x' - a_y')(\sigma_x' - \sigma_y') - (a_x'' - a_y'')(\sigma_x'' - \sigma_y''),\end{aligned} \tag{11}$$

Table 2
Values of coefficients in eqs. (9) and (10) for Cu(110), $\Omega = 0°$, $\phi_0 = 66°$

λ (nm)	a'_x	$-a'_y$	a'_z	$-a''_x$	a''_y	a''_z	b'_x	$-b'_y$	$-b'_z$	b''_x	$-b''_y$	b''_z
460	0.34	0.07	2.35	0.17	0.06	0.88	0.08	0.03	0.42	0.16	0.03	1.11
500	0.29	0.06	2.23	0.15	0.05	0.75	0.07	0.02	0.36	0.14	0.03	1.06
560	0.29	0.07	1.83	0.08	0.03	0.43	0.04	0.02	0.21	0.14	0.03	0.90
600	0.23	0.05	1.93	0.01	0.00	0.06	0.01	0.00	0.03	0.12	0.03	0.97
640	0.18	0.04	2.01	0.01	0.00	0.03	0.00	0.00	0.01	0.09	0.02	1.00
700	0.12	0.02	2.07	0.00	0.00	0.02	0.00	0.00	0.01	0.06	0.01	1.04
760	0.10	0.02	1.97	0.00	0.00	0.02	0.00	0.00	0.01	0.05	0.01	0.98

$$\delta\bar{\psi} \equiv \bar{\psi}\,(\Omega = 0°) - \bar{\psi}\,(\Omega = 90°)$$
$$= -(b_x' - b_y')(\sigma_x' - \sigma_y') - (b_x'' - b_y'')(\sigma_x'' - \sigma_y''). \quad (12)$$

Calculated values of the coefficients in eq. (9) and (10) for Cu(110) at $\Omega = 0°$ are given in table 2 for a few wavelengths. For Cu(110) at $\Omega = 90°$ some coefficients show a small deviation in the second place of decimals, particularly at higher wavelengths. The coefficients a_y', a_x'', b_y', b_z' and b_y'' are negative and the absolute values of a_j' and b_j'' turn out to be larger than those of a_j'' and b_j', respectively, especially at longer wavelengths. From the values of the coefficients it follows that differences in $\delta\Delta$, and also in $\delta\bar{\Delta}$, are primarily associated with differences in σ_j', and differences in $\delta\psi$ and $\delta\bar{\psi}$ mainly with differences in σ_j''.

For example, the large value of $\delta\bar{\Delta}$ at $\lambda \approx 640$ nm (fig. 5) would imply $\sigma_x' < \sigma_y'$, i.e. a smaller σ' (and α') in the direction parallel to the rows than perpendicular to them. If the absolute values of $\delta\bar{\Delta}$ and $\delta\bar{\psi}$ were reliable, one could even calculate the differences $(\sigma_x' - \sigma_y')$ and $(\sigma_x'' - \sigma_y'')$ with eqs. (11) and (12).

4. Interaction of oxygen with clean copper surfaces

Exposures of O_2 to clean annealed copper surfaces were carried out at pressures between 10^{-7} and 10^{-3} Torr and at crystal temperatures ranging from 295 to 620 K. Fig. 6 shows a typical plot of the change in the ellipsometric parameters Δ and ψ during room temperature exposure of oxygen to

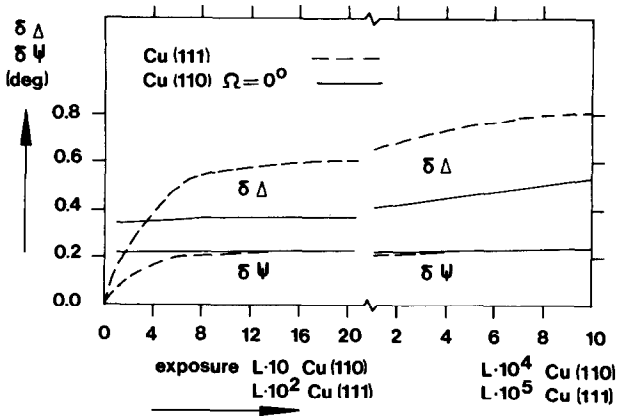

Fig. 6. $\delta\Delta$ and $\delta\psi$ as a function of oxygen exposure. Oxygen pressures for Cu(110), $\Omega = 0°$: 1.2×10^{-7} and 1.2×10^{-4} Torr; for Cu(111): 2×10^{-6} and 10^{-3} Torr. Wavelength: 632.8 nm, $\phi_0 = 66°$.

Cu(110) and Cu(111) at $\lambda = 632.8$ nm. As found before by Habraken et al. [4], the initial interaction of oxygen with the copper surfaces occurs in two stages. In the first stage, at low oxygen pressures, ellipsometric parameters tend to almost constant saturation values, which are reached at about 10^2 L for Cu(110) and 2×10^3 L for Cu(111).

According to Habraken et al., the oxygen coverages are then equal to 0.5 [3] and 0.45 [1] monolayers, respectively. An increase of the oxygen pressure leads to a further, continuing change in Δ and ψ. Though somewhat arbitrarily, we have chosen exposure values of 10^5 L for Cu(110) [4] and of 10^6 L for Cu(111) to represent the monolayer coverage situation.

4.1. The Cu(111) surface

In fig. 7, the changes of the ellipsometric parameters Δ and ψ are given as a function of the wavelength for the two oxygen exposures at different sample temperatures. The exposures at 10^{-3} Torr was only performed at room temperature. The measurements were carried out at the same two azimuths of the plane of incidence as for clean Cu(111) (cf. section 3.1). Within the experimental error, the values of $\delta\Delta$ and $\delta\psi$ appeared to be independent of Ω. The shapes of the $\delta\Delta(\lambda)$ and $\delta\psi(\lambda)$ curves turned out to be the same for the two exposures and the different temperatures.

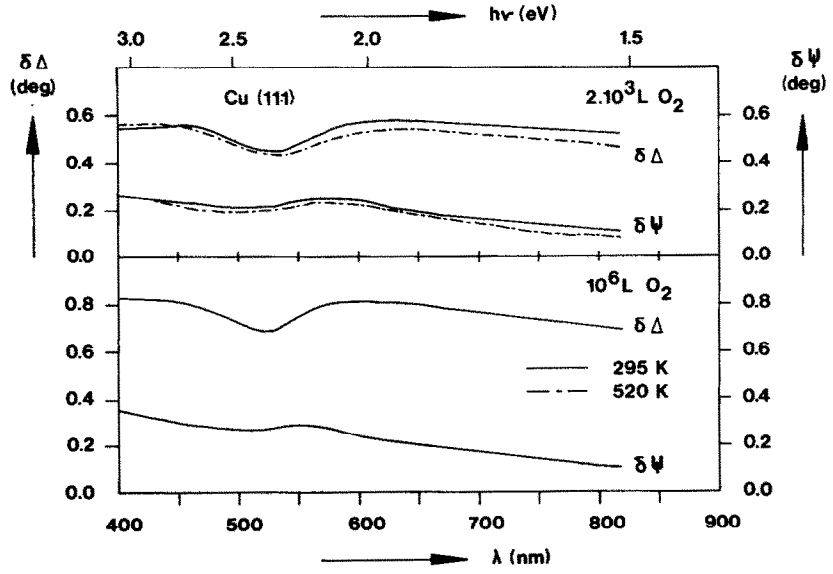

Fig. 7. Ellipsometric effects measured upon adsorption of oxygen on Cu(111), oxygen pressures 2×10^{-6} and 10^{-3} Torr, $\phi_0 = 66°$.

4.2. The Cu(110) surface

The spectroscopic ellipsometry plots for 10^2 L and 10^5 L oxygen exposures are given in fig. 8 for $\Omega = 0°$ and in fig. 9 for $\Omega = 90°$. In contrast with the Cu(111) surface, the $\delta\Delta$ and $\delta\psi$ values appear to be strongly dependent on the azimuth of the plane of incidence, particularly at wavelengths from 500 to 700 nm, i.e. in the absorption band region of copper. Besides these differences in structure the $\delta\Delta$ values tend to be larger for $\Omega = 90°$.

An increase of the oxygen exposure causes mainly a rise of $\delta\Delta$, while the shapes of the curves remain similar. At 10^5 L exposure the $\delta\Delta(\lambda)$ curve for $\Omega = 90°$ shows an increase at higher temperature, particularly at longer wavelength, outside the absorption band region. The $\delta\psi$ values appear to be almost independent of temperature and oxygen exposure.

Comparison of figs. 7 and 8 shows that the shapes of the curves for Cu(111) and Cu(110), $\Omega = 0°$, are rather similar but that the absolute values of the ellipsometric changes are larger for Cu(111).

4.3. Anisotropy of oxygen covered Cu(110)

The differences in $\delta\Delta$ and $\delta\psi$, measured for the two orientations of the plane of incidence, can be written as

$$\delta(\delta\Delta) = \delta\bar{\Delta} - [\Delta(\Omega = 0°) - \Delta(\Omega = 90°)], \tag{13}$$

$$\delta(\delta\psi) = \delta\bar{\psi} - [\psi(\Omega = 0°) - \psi(\Omega = 90°)]. \tag{14}$$

In contrast with the absolute measurements on clean surfaces, yielding $\delta\bar{\Delta}$ and $\delta\bar{\psi}$, the relative measurements of the changes upon adsorption, yielding $\delta(\delta\Delta)$ and $\delta(\delta\psi)$ (fig. 10), are reliable, because the effect of window birefringence is negligible for small values of $\delta\Delta$ and $\delta\psi$.

In principle, the structure of the curves in fig. 10 may be due to anisotropy of the clean Cu(110) surface and/or to anisotropy in the distribution of the chemisorbed oxygen atoms or in the copper–oxygen bonds. The similarity of figs. 5 and 10 suggests that the differences in the $\delta\Delta$ and the $\delta\psi$ curves may, at least partially, be ascribed to a disappearance of the anisotropy of clean Cu(110) upon oxygen adsorption. A comparison of the absolute values of the corresponding curves is not useful, because the absolute values of $\delta\bar{\Delta}$ and $\delta\bar{\psi}$ are open to doubt.

If we would ascribe the experimental results totally to anisotropy in the final surface oxide layer, Strachan's approach could be applied, as was done by Habraken et al. [5] for $\lambda = 632.8$ nm. In view of the values of the coefficients of eqs. (11) and (12), derived from table 2, the $\delta(\delta\Delta)$ curves in fig. 10 represent mainly $(\sigma_x' - \sigma_y')$ and the $\delta(\delta\psi)$ curves mainly $(\sigma_x'' - \sigma_y'')$, assuming that the components σ_i' and σ_i'' are of the same order of magnitude in both directions. From this it follows that $\sigma_x' < \sigma_y'$, with a strong variation of $(\sigma_x' - \sigma_y')$ in the

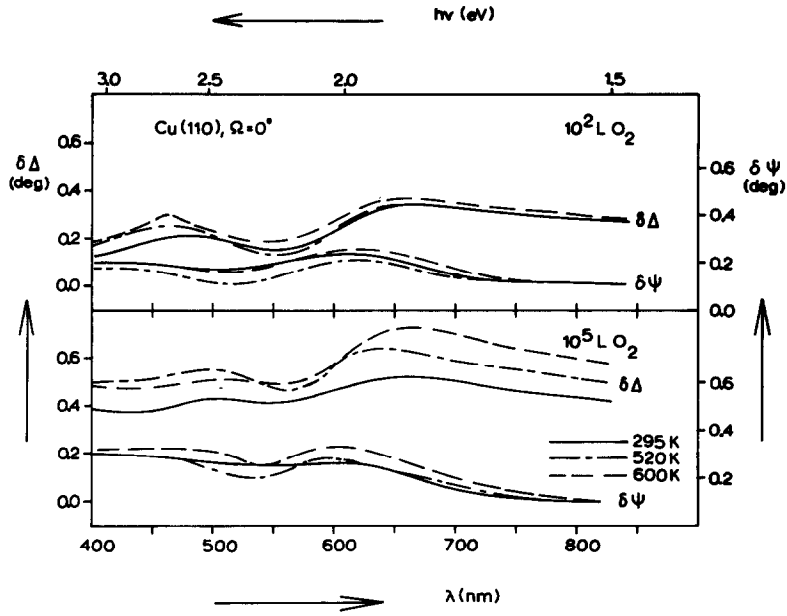

Fig. 8. Ellipsometric effects measured upon adsorption of oxygen on Cu(110), $\Omega = 0°$, oxygen pressures 1.2×10^{-7} and 1.2×10^{-4} Torr, $\phi_0 = 66°$.

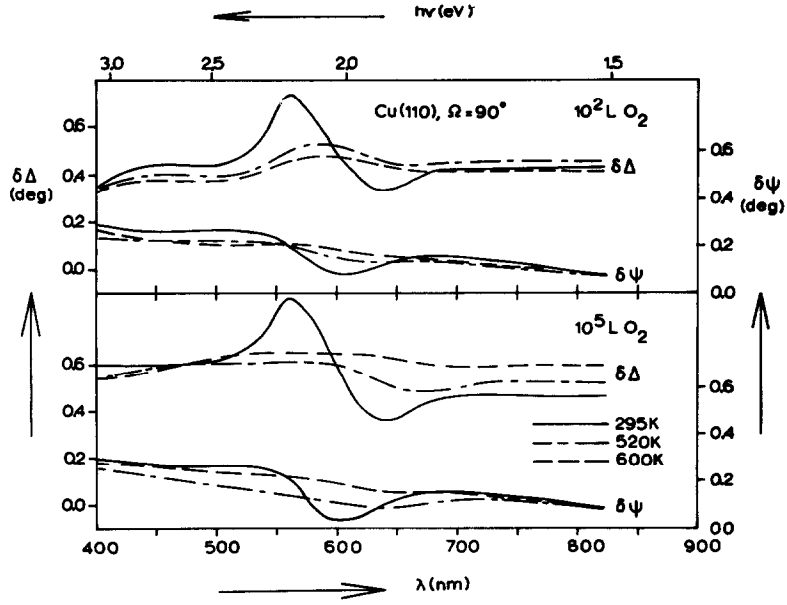

Fig. 9. Ellipsometric effects measured upon adsorption of oxygen on Cu(110), $\Omega = 90°$, oxygen pressures 1.2×10^{-7} and 1.2×10^{-4} Torr, $\phi_0 = 66°$.

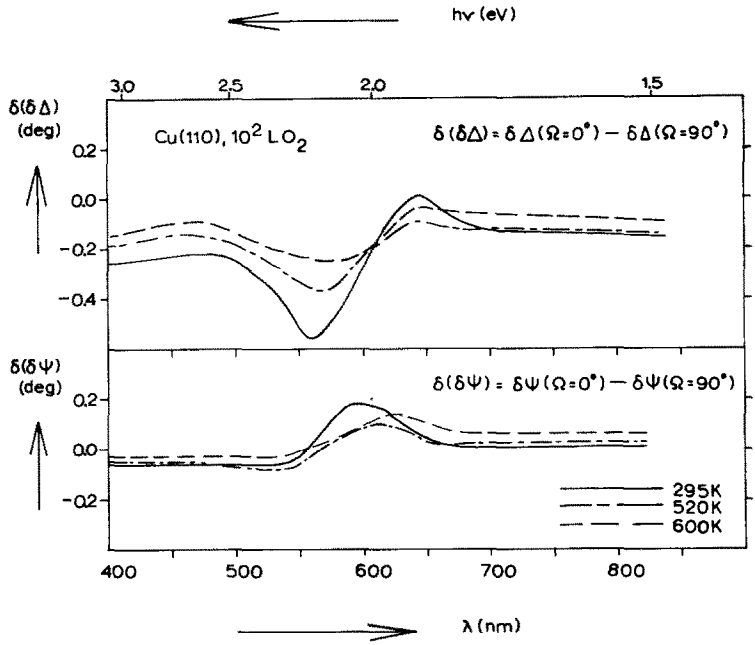

Fig. 10. Difference in ellipsometric effects $\delta\Delta$ and $\delta\psi$ measured for Cu(110) at $\Omega = 0°$ (fig. 8) and 90° (fig. 9) after 10^2 L oxygen exposure.

band region. The difference $(\sigma_x'' - \sigma_y'')$ is almost zero except in the band region, where $\sigma_y'' > \sigma_x''$. Increase of the temperature reduces the differences.

4.4. Models of oxygen covered copper surfaces

To account for the ellipsometric results the three models discussed by Habraken et al. [5] to explain the measurements at 632.8 nm were applied.

(a) The model used for the interpretation of the ellipsometric results for chemisorption on semiconductor surfaces [27], where the main effect is ascribed to the disappearance of a surface layer at the clean surface. Calculations with this model did not yield physically reasonable values for the optical constants of the surface layer.

(b) The one-layer model with formation of a surface oxide with effective dielectric constant $\tilde{\epsilon}$ and thickness d_1. With the computer program of McCrackin [12], the components ϵ' and ϵ'' were calculated from the Δ, ψ values measured at the end of the chemisorption stage by taking $d_1 = 2$ Å [5]. For Cu(110) the components of $\tilde{\epsilon}$ show a strong oscillatory character at $\Omega = 90°$ and a weak at $\Omega = 0°$, while for Cu(111) a gradual increase with increasing

wavelength occurs. These results differ strongly from the literature values of Cu_2O (cf. fig. 11).

(c) The two-layer model with adsorbed oxygen ions on top of an effectively positively charged metal surface layer, caused by a decrease of the free electron density. Because the changes in the ellipsometric parameters vary strongly in the absorption band region of copper, an explanation based only on changes in the contribution of the free electrons seems inadequate.

The effective medium approximation (EMA) due to Bruggeman [28] gives a possibility to take into account the bound electrons in copper. The first stage of oxidation of Mg(001), investigated by Kötz et al. [29] using spectroscopic ellipsometry, was described in terms of the growth of a surface layer consisting of a mixture of bulk Mg and MgO of which the dielectric constant was calculated with the EMA. A detailed description of the EMA has been given by Aspnes et al. [30–32]. The EMA formulation for a medium of two components, where the effective medium itself acts as host medium is

$$f\frac{\epsilon_1-\langle\epsilon\rangle}{\epsilon_1+2\langle\epsilon\rangle}+(1-f)\frac{\epsilon_2-\langle\epsilon\rangle}{\epsilon_2+2\langle\epsilon\rangle}=0, \tag{15}$$

where $\langle\epsilon\rangle$, ϵ_1 and ϵ_2 are the complex dielectric functions of the effective medium, components 1 and 2, and f the volume fraction of component 1.

Results calculated for layers of Cu_2O and for mixtures of Cu and Cu_2O are

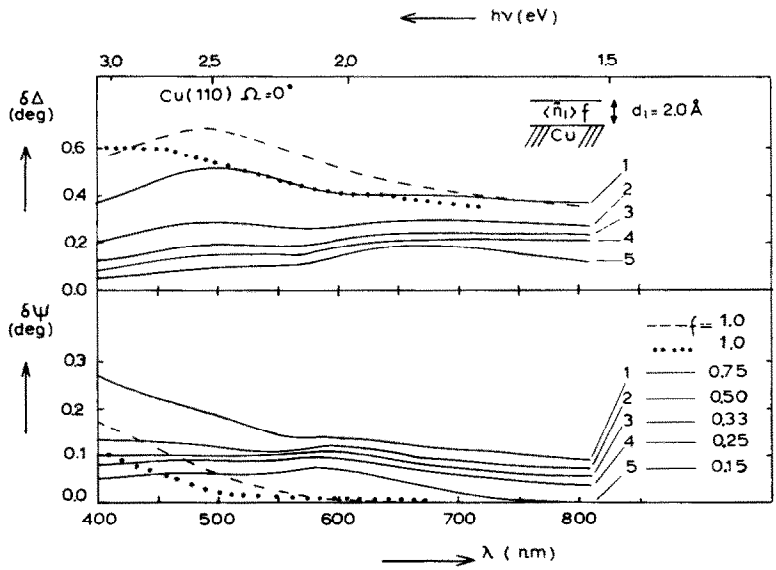

Fig. 11. Ellipsometric effects calculated for layers of Cu_2O (— — —, ref. [34]; ·····, ref. [33]) and of mixtures of Cu and Cu_2O (f: volume fraction of Cu_2O) on clean Cu(110), $\Omega=0°$, $\phi_0=66°$.

given in fig. 11; the thickness was arbitrarily chosen equal to 2 Å; another choice does not influence the shape but only the height of the curves. The optical constants of Cu_2O were taken from recent measurements on films grown on copper [33] and on reactivily-sputtered thin films [34]. The effective dielectric constants of mixtures were calculated with eq. (15), by taking for ϵ_1 the values of Drobny and Pulfrey [34] and for ϵ_2 those measured for clean Cu(110) at $\Omega = 0°$. Equivalent results were obtained by taking for ϵ_2 values measured for clean Cu(111).

Comparison with the experimental curves of figs. 7, 8 and 9 shows that apparently the optical properties of the surface oxide are quite different from those of "bulk" Cu_2O. Better but not yet satisfactory agreement is found with the EMA results for mixtures of Cu and Cu_2O, at least for Cu(110) at $\Omega = 0°$ and Cu(111). However, with this model it is impossible to describe the results for Cu(110) at $\Omega = 90°$, even with ϵ_2 values measured for clean Cu(110) at 90°.

Acknowledgement

The authors would like to thank Th.L. Schroote (State University of Utrecht) for the preparation of the samples and K.O. van der Werf for the technical assistance.

References

[1] F.H.P.M. Habraken, E.Ph. Kieffer and G.A. Bootsma, Surface Sci. 83 (1979) 45.
[2] F.H.P.M. Habraken, C.M.A.M. Mesters and G.A. Bootsma, Surface Sci. 97 (1980) 264.
[3] F.H.P.M. Habraken and G.A. Bootsma, Surface Sci. 87 (1979) 333.
[4] F.H.P.M. Habraken, G.A. Bootsma, P. Hofmann, S. Hachicha and A.M. Bradshaw, Surface Sci. 88 (1979) 285.
[5] F.H.P.M. Habraken, O.L.J. Gijzeman and G.A. Bootsma, Surface Sci. 96 (1980) 482.
[6] O. Oda, L.J. Hanekamp and G.A. Bootsma, Appl. Surface Sci. 7 (1981) 206.
[7] R.W. Stobie, B. Rao and M.J. Dignam, J. Opt. Soc. Am. 65 (1975) 25.
[8] R.W. Stobie, B. Rao and M.J. Dignam, Appl. Opt. 14 (1975) 999.
[9] A. Straayer, L.J. Hanekamp and G.A. Bootsma, Surface Sci. 96 (1980) 217.
[10] F.L. McCrackin, E. Passaglia, R.R. Stromberg and H.L. Steinberg, J. Res. Natl. Bur. Std. 67A (1963) 363.
[11] F.C. Schouten, E.W. Kaleveld and G.A. Bootsma, Surface Sci. 63 (1977) 460.
[12] F.L. McCrackin, FORTRAN Program for Analysis of Ellipsometer Measurements (Natl. Bur. Std. (US) Tech. Note 479, Washington, DC, 1969).
[13] S. Roberts, Phys. Rev. 118 (1960) 1509.
[14] M.Ph. Stoll, J. Appl. Phys. 40 (1969) 4533.
[15] G.P. Pells and M. Shiga, J. Phys. C2 (1969) 1835.
[16] P.B. Johnson and R.W. Christy, Phys. Rev. B6 (1972) 4370.
[17] P.B. Johnson and R.W. Christy, Phys. Rev. B11 (1975) 1315.
[18] U. Merkt and P. Wissmann, Thin Solid Films 57 (1979) 65.
[19] H. Bispinck, Z. Naturforsch. 25A (1970) 70.

[20] J.V. Cathcart and G.F. Petersen, in: Ellipsometry in the Measurement of Surfaces and Thin Films, Eds. E. Passaglia, R.R. Stromberg and J. Kruger (Natl. Bur. Std. (US) Misc. Publ. 256, Washington, DC, 1964) p. 201.
[21] T.E. Furtak and D.W. Lynch, Phys. Rev. Letters 35 (1975) 960.
[22] R. Kofmann, P. Cheyssac and J. Richard, Surface Sci. 77 (1978) 537.
[23] R. Kofmann, R. Garrigos and P. Cheyssac, Surface Sci. 101 (1980) 231.
[24] A. Tadjeddine, D.M. Kolb and R. Kötz, Surface Sci. 101 (1980) 277.
[25] R.E. Hummel, Optische Eigenschaften von Metallen und Legierungen (Springer, Berlin, 1971).
[26] C. Strachan, Proc. Cambridge Phil. Soc. 29 (1933) 116.
[27] G.A. Bootsma and F. Meyer, Surface Sci. 14 (1969) 52.
[28] D.A.G. Bruggeman, Ann. Physik (Leipzig) 24 (1935) 636.
[29] R. Kötz, B. Hayden, E. Schweizer and A.M. Bradshaw, Surface Sci., to be published.
[30] D.E. Aspnes, J.B. Theeten and F. Hottier, Phys. Rev. B20 (1979) 3292.
[31] D.E. Aspnes and J.B. Theeten, Phys. Rev. Letters 43 (1979) 1046.
[32] D.E. Aspnes, E. Kinsbron and D.D. Bacon, Phys. Rev. B21 (1980) 3290.
[33] K. Bärwinkel and H.J. Schmidt, Thin Solid Films 59 (1979) 373.
[34] V.F. Drobny and D.L. Pulfrey, Thin Solid Films 61 (1979) 89.